

# TUNNELING INTO RESISTIVE MULTIWALLED CARBON NANOTUBES

R. TARKIAINEN, M. AHLKOG, L. ROSCHIER, P. HAKONEN, and M. PAALANEN  
*Low Temperature Laboratory, Helsinki University of Technology, FIN-02015 HUT, Finland*

We have studied electron tunneling between CVD-grown multiwalled carbon nanotube and gold contact in 2-lead and 4-lead measurement geometries with wide contact pads. We have compared the observed zero bias anomaly in tunneling conductance with the predictions of Luttinger liquid, 1D diffusion and coherent conductor models. We will discuss the validity of different models and the implications of their fitting parameters.

## 1 Introduction

Carbon nanotube is an interesting realization of one dimensional electrical conductor<sup>1,2</sup>. It is made out of long coaxial cylinders of graphene sheets which are decoupled from each other but conduct along their axis. The electrical properties of a single cylinder can be derived from the band structure of graphite and one finds both metallic and semiconducting behavior. As in ordinary semiconductors, one can also manipulate the conductivity of carbon nanotubes by doping.

In a truly one dimensional conductor electron backscattering, which requires a large momentum change, is a relatively rare event. In addition, one can apparently quite easily produce nearly defect free single walled nanotubes with low intrinsic impurity concentration. Consequently, one expects SWNTs to be excellent 1D conductors with nearly ballistic electron motion. Several experiments support this picture<sup>3,4,5,6</sup>. SWNTs are found to carry high current densities at higher voltages. Also, tunneling experiments with SWNTs can be explained with the Luttinger liquid model<sup>7,8</sup> which is valid for ballistic, strongly interacting electron gas<sup>9,10,11</sup>. The conductance of an ideal 1D conductor should also be quantized. For undoped metallic SWNTs, containing 4 independent conduction channels, the value of the quantized conductance is expected to be  $4e^2/h$ . However, accurate measurement of this value requires ideal low ohmic contacts, which have turned out to be difficult to make. A clean metal-nanotube interface acts as a tunneling barrier which, however, is useful for studying single electron density of states of the nanotubes<sup>7</sup>.

Electrical properties of multiwalled nanotubes are somewhat less understood<sup>12</sup>. Role of inner layers, number of conducting channels, disorder strength, and carrier concentrations in these samples can vary over a wide range and are hard to control experimentally. The inner cylinders are capacitively coupled to the outer layer and participate only in the high frequency conductivity. Compared to single walled nanotubes, the larger diameter and screening by inner layers is expected to reduce electron-electron and presumably also electron-impurity scattering in the MWNTs. Otherwise, the electrical properties of MWNTs and SWNTs should be quite similar. Recent magnetoresistance measurements have confirmed that only the outermost graphene cylinder conducts but the mean free path of the electrons is quite short, less than 100 nm<sup>13,14</sup>. Presumably, high quality MWNTs are more difficult to produce than SWNTs and have a higher defect density per unit length. Also, the unmatched lattices of the inner layers may act as intrinsic scattering potential for electrons on the outermost layer. Due to large scattering the Luttinger liquid model is not expected to work well for MWNTs.

In this work we have studied tunneling density of states for CVD-grown multiwalled nanotubes by measuring the conductance of gold-nanotube tunnel junctions. After tunneling the electron has to penetrate Coulomb barrier, a time-dependent self energy which reduces the tunneling probability<sup>15,16</sup>. The self-energy has maximum value just after the tunneling and decreases as soon as the electron charge is redistributed in the nanotube. Thus, the tunneling density of states is a direct measure of the impedance of the nanotube. The impedance of ballis-

tic and diffusive nanotubes can be obtained from the impedance of inductive (LC) and resistive (RC) transmission lines, respectively.

## 2 Sample Preparation

We have prepared three over 2  $\mu\text{m}$  long nanotube samples for the conductivity measurements. The nanotubes, grown by chemical vapour deposition (CVD), were multiwalled, with an initial diameter of about 18 nm. Compared to the arc discharge (AD) grown nanotubes, the CVD tubes have more curvature and bends, implicating a higher density of structural defects. These defects may act as scattering centers and increase the resistance of the tubes.

One of the nanotubes, later named as CVD sample, was deposited across two pre-evaporated gold contacts. The two other samples, RIE1 and RIE2, were first deposited on the substrate and reactive ion etched down to a diameter of 10 nm, before the evaporation of the gold leads. Normally, one expects the RIE treatment to damage conducting samples and increase their resistance. The evaporation of contact metal on the top of the nanotube may have a similar effect. In addition, metals and nanotubes have usually different electron work functions which may lead to considerable doping of the nanotube by the contact metal. In case of gold, the contact doping is expected to be p-type.

The metal-nanotube contacts are tunnel junctions, whose microscopic structure is not well understood. However, our long junction may be parametrized by a distributed tunneling conductance and capacitance of the order of 100  $\mu\text{S}/\mu\text{m}$  and 100 aF/ $\mu\text{m}$ , respectively. These values are valid for contacts formed on the top of the metal by the van der Waals force. A larger conductance and capacitance can be expected for junctions buried inside or under the metal. In case of single walled nanotubes, large differences have been detected between the top and buried contacts<sup>7</sup>. All our junctions were about 1  $\mu\text{m}$  long and the gold electrodes were separated by a narrow gap (Fig. 1). Consequently, our resistance measurements are probing the properties of the nanotube in close contact with the gold.

## 3 Results

The samples were cooled down in a dilution refrigerator and their  $I$  vs  $V$  and conductance  $G$  vs  $V$  curves were measured from -100 to 100 mV from liquid He temperature down to 130 mK. In our 2-lead measurement geometry with wide contact pads, the resistance of the sample contains series resistance of the two long tunneling contacts. In the following analysis we will assume identical contacts, which dominate the resistance, and compare our data with the predictions of Luttinger liquid<sup>17,18,19</sup> and diffusive conductor models<sup>20,21,22</sup>. The resistance measured in 4-lead geometry is assumed to be dominated by the resistance of the nanotube, and these results will be compared with the coherent conductor model<sup>23,24</sup>.

A clean interacting 1D electron gas is expected to behave like a Luttinger liquid (LL). A Fermi liquid has single electron excitations moving with the Fermi velocity  $v_F$ . In contrast, due to the repulsive e-e interaction, the low energy excitations of a LL are plasmas whose velocity  $v_{pl} > v_F$ . For our tunneling geometry, so called bulk tunneling geometry, the tunneling conductance is predicted to have a zero bias suppression  $G \propto V^\alpha$  where  $\alpha = (v_{pl}/v_F + v_F/v_{pl} - 2)/2M$ , and  $M$  the number of independent conduction channels in the nanotube<sup>10,11,7</sup>. If the nanotube is modeled as an LC transmission line then  $v_{pl} = 1/\sqrt{lc}$ , where  $l$  and  $c$  are the kinetic inductance and effective capacitance per unit length, respectively<sup>19</sup>. Thus, the zero bias anomaly is a sensitive function of e-e interactions ( $v_{pl}$ ), doping level of the nanotube ( $v_{pl}, M$ ) and the capacitance of the junction ( $c$ ).

In Figure 1 we have tested our low temperature ( $eV \gg k_B T$ ) conductance data against the LL model, which predicts a linear  $\ln G$  vs  $\ln V$  dependence. For a single tunnel junction in a finite

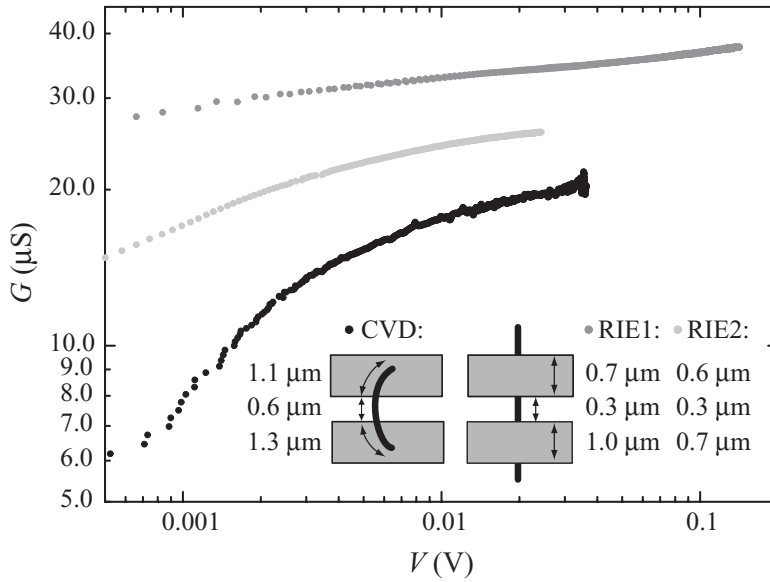


Figure 1: Test of Luttinger liquid model for three CVD-grown samples in low temperature limit  $eV > k_B T$ . According to the Luttinger liquid theory,  $\ln G \propto \alpha \ln V$  above the plasmon energy at  $eV \sim 2$  meV for two tunnel junctions in series. At higher voltages the model is limited by the lowest transverse mode of the nanotube at about 120 mV for RIE1 and RIE2 and 70 mV for the CVD-grown sample. Linear behavior is observed at higher voltages, but with unexpectedly small values of exponent  $\alpha$ .

length nanotube, the LL model is expected to be valid over an energy interval from the plasmon energy  $eV = \hbar v_{pl}/2L = 1$  meV to the lowest transverse mode energy  $eV = \hbar v_F/\pi\phi = 60$  meV. These values are calculated for a tube whose length  $L = 1 \mu\text{m}$ , diameter  $\phi = 10$  nm,  $v_F = 8 \cdot 10^5$  m/s and  $v_{pl} = 3 \cdot 10^6$  m/s. Our data is not linear over the predicted voltage window. If we, however, extract an exponent  $\alpha$  at the highest voltages, it turns out to be 0.05 - 0.15, an unexpectedly small number. One might explain the small values of  $\alpha$  by a high value of capacitance  $c$  of the gold-nanotube tunnel junction or by a high carrier concentration (large  $M$ ) of the part of the nanotube which is in contact with the gold, *i.e.* by a strong doping effect of the gold. Also, strong tunneling effects may reduce the values of  $\alpha$ . In contrast to the SWNT tunneling measurements<sup>7</sup>, our  $\alpha$  values are larger for the top contact than for the buried contact. Also, the increase of the  $\alpha$  values with increasing tube diameter, *i.e.* with increasing number of conduction channels, is hard to understand.

Due to high anticipated resistance of the CVD tubes, it is natural to test our data against the predictions of the 1D diffusion model<sup>20,22</sup>. In this model, the leading low temperature correction to the tunneling conductance is proportional to  $-\sqrt{V_o/V}$ . This prediction is tested in Fig. 2 by plotting  $\ln G(V)$  against  $1/\sqrt{V}$ . According to Fig. 2,  $G(V) = G_o \exp(-\sqrt{V_o/V})$ , which actually goes beyond the leading order prediction of the diffusion model and deviates from recent higher order predictions in Refs. 16,21. The parameter  $V_o = (r/R_K)(e/\pi c)$  can be determined from the linear fits in Fig. 2<sup>22</sup>. In this formula the resistance quantum  $R_K = h/e^2$ . Assuming that  $c = 100$  aF/ $\mu\text{m}$  for the top and and 300 aF/ $\mu\text{m}$  for the buried contact, we obtain quite reasonable values of 5 - 30 k $\Omega/\mu\text{m}$  for the line resistance  $r$ . Interestingly, the RIE treatment seems to reduce  $r$  which may indicate that the RIE is removing complete layers at once and the inner layers have less structural defects.

The demarcation line between 1D and 2D diffusion models is located at tunneling energy  $eV = \hbar D^*/(\pi\phi)^2 > 100$  meV for all our tubes<sup>22</sup>. The dimensionality of the sample is determined by  $D^* = 1/rc \sim .1-1$  m<sup>2</sup>/s, the diffusion constant of the electric field rather than by  $D$ , the diffusion constant of single electrons. At lower voltages  $eV < \hbar D^*/(L/2)^2 \sim 3$  meV the diffusion

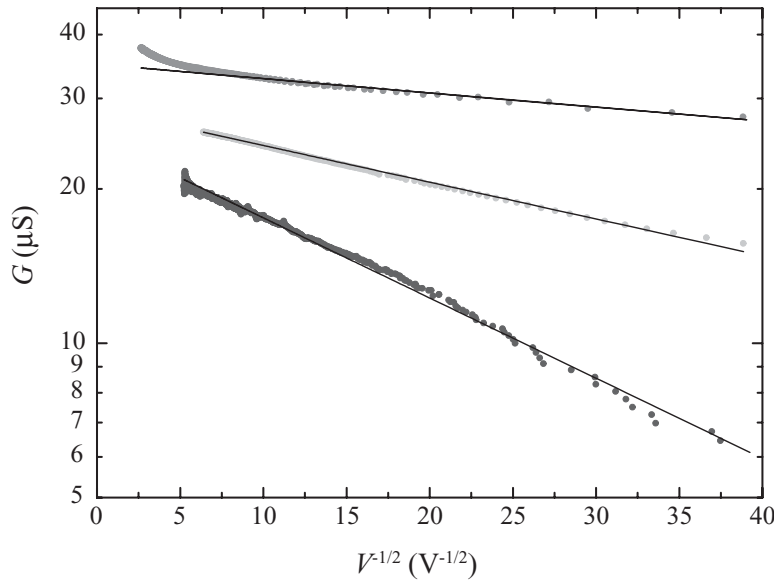


Figure 2: Test of 1D-diffusion model at low temperatures  $eV \gg k_B T$ . The diffusion model fits the data of all three nanotubes over a wide voltage range with reasonable fitting parameters.

model breaks down and should be replaced by the coherent conductor model<sup>23</sup>. Except for the RIE1 sample at high voltages, the diffusion model gives an excellent fit to our data over a wide voltage range. The small upward curvature in the RIE1 data could be explained either by a  $V^3$  correction to the tunneling probability or by the closeness of the lowest transverse mode at  $V = 120$  mV ( $2 \times 60$  mV).

In an ideal 4-lead geometry one is measuring the resistance of a sample between narrow voltage contacts, *i.e.* without the contact resistances. The fact that the zero bias anomaly is also visible in our 4-lead measurement may result from the zero bias anomaly in the 1D conductivity of the nanotube<sup>20,23</sup> or, in our long contact geometry, from the tunneling of electrons through the low ohmic path, provided by the voltage leads. In the following we will assume the previous case and analyze our results with the coherent conductor model<sup>23</sup>. In this model the zero bias anomaly of a 1D conductor, containing several parallel conduction channels with transmission coefficients  $T_i$  and total resistance  $R = h/e^2 \Sigma T_i$ , results from the e-e interactions. The interactions are parametrized by a phenomenological Coulomb energy  $E_c$ . This model has several restrictions which may not be fulfilled for our samples. The conductor is assumed to be shorter than the coherence length of diffusing electrons, and isolated from the voltage source by a shunt resistance  $R_s$ . The model works only in the high conductance limit of  $g_0 = R_K/R + R_K/R_s \gg 1$ , and for  $\max(eV, k_B T) > g_0 E_c \exp(-g_0/2)$ . At the same time the measuring voltage cannot exceed the Thouless energy of  $eV = \hbar D/L^2$ .

The coherence length requirement can presumably be fulfilled at our lowest measurement temperatures. In our samples the tunneling resistors act as  $R_s$ , but unfortunately we cannot determine their values independently. Despite of these shortcomings, we have tested the model in Figure 3 for RIE2 sample in 4-lead geometry. A reasonable fit to our data is found with the parameters  $R = 34.5$  k $\Omega$ ,  $R_s = 5$  k $\Omega$ ,  $g_0 = 5.9$ ,  $\beta = \Sigma T_i(1 - T_i)/\Sigma T_i = 0.1$  and  $E_c = 109$  K. However, the fit is obtained in the low temperature and low voltage limit ( $eV, k_B T$ )  $< g_0 E_c \exp(-g_0/2)$ , where the theory is not supposed to work. The parameters turn out to be quite reasonable except that the value of  $\beta$  is too small and the Coulomb energy far too large. For a diffusive 1D conductor  $\beta$  is expected to be 0.33.

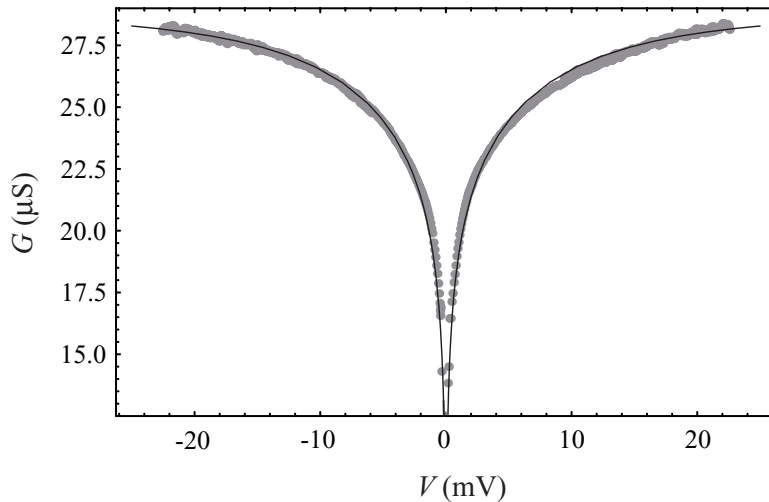


Figure 3: Test of coherent conductor model in RIE2 at  $T = 130$  mK. This model fits the conductivity data quite well up to about 20 mV but fails, as expected, at higher voltages. However, the fitting parameters of this model turn out to be somewhat unphysical.

## 4 Summary

A nanotube can be modeled as an inner conductor of a transmission line whose outer conductor is formed by nearby metallic objects. In an usual measurement geometry, the ends of a nanotube are in short tunnelling contact with metallic pads while the long middle section rests on a semiconducting substrate, resulting in capacitance, electron density and ultimately impedance variations along the nanotube. The impedance and its variations can be studied by measuring the voltage dependent tunneling conductance of the contacts.

We have studied conductance of three CVD grown multiwalled nanotubes in 2-lead and 4-lead measurement geometries, with wide contact pads positioned close to each other. In the 2-lead geometry, the resistance of the sample is assumed to be essentially the series resistance of two identical tunneling contacts. We have compared our data with the two available theoretical models for electron motion in a transmission line: ballistic (LC transmission line) and diffusion model (RC transmission line). At high voltages, the tunneling current measures the impedance of the nanotube in intimate contact with gold contact while the impedance of the whole sample is probed at lower voltages. We find over a wide voltage range that the diffusion model explains our results with reasonable fitting parameters. The domination of the RC over the LC model may be justified by the large resistance  $R$  of the CVD grown nanotubes, and presumably by the reduced kinetic inductance  $L$ , *i.e.* enhanced carrier concentration of the nanotube in contact with gold. We obtain a rough estimate of  $30 \text{ k}\Omega/\mu\text{m}$  for the resistance of the untreated CVD tube. Unexpectedly, reactive ion etching is found to reduce the resistance by about factor five.

In our 4-lead measurements we have assumed to probe the resistance of the nanotube without contact resistances and have analyzed the results with the coherent conductor model. We have found a good fit to the data, but with somewhat unphysical values of the fitting parameters.

## Acknowledgments

Fruitful discussions with Boris Altshuler, Leonid Glazman, Frank Hekking, Edouard Sonin, Boris Spivak and Andrei Zaikin are gratefully acknowledged. We also thank Dr. A. Fonseca and Prof. J.B. Nagy from the Universitaires Notre-Dame de la Paix Namur, for providing us with the nanotubes in this work. This work was supported by the Academy of Finland and by ULTI III,

## References

1. See, *e.g.*, "Special Issue on Nanotubes" in *Physics World*, June 2000, p. 29.
2. C. Dekker, *Physics Today*, May 1999, p. 22.
3. S.J. Tans, M.H. Devoret, H. Dai, A. Thess, T.E. Smalley, L.J. Geerligs, and C. Dekker, *Nature* **386**, 474 (1997).
4. M. Bockrath, D.H. Cobden, P.L. McEuen, N.G. Chopra, A. Zettl, A. Thess, and R.E. Smalley, *Science* **275**, 1922 (1997).
5. J. Kong, C. Chou, A. Morpurgo, H.T. Soh, C.F. Quate, C. Marcus, and H. Dai, *Appl. Phys. A* **69**, 305 (1999).
6. A. Bachtold, M.S. Fuhrer, S. Plyasunov, M. Forero, E.H. Anderson, A. Zettl, and P.L. McEuen, *Phys. Rev. Lett.* **84**, 6082 (2000).
7. M. Bockrath, D.H. Cobden, J. Lu, A.G. Rinzler, R.E. Smalley, L. Balents, and P.L. McEuen, *Nature* **397**, 598 (1999).
8. Z. Yao, H. W. Ch. Postma, L. Balents, and C. Dekker, *Nature* **402**, 273 (1999).
9. See, *e.g.*, M.P.A. Fischer and L.I. Glazman in *Mesoscopic Electron Transport*, edited by L.L. Sohn, L.P. Kouwenhoven, and G. Schön (Kluwer Academic Publishers, Dordrecht, 1997) p. 331; J. Voigt, cond-mat/0005114.
10. R. Egger, and A. Gogolin, *Phys. Rev. Lett.* **79**, 5082 (1997)
11. C. Kane, L. Balents and M.P.A. Fisher, *Phys. Rev. Lett.* **79**, 5086 (1997).
12. R. Tarkiainen, M. Ahlskog, J. Penttiä L. Roschier, P. Hakonen, M. Paalanen, and E. Sonin, cond-mat/0104019.
13. L. Langer, V. Bayot, E. Grivei, J.-P. Issi, J.P. Heremans, C.H. Olk, L. Stockman, C.V. Haesendonck, and Y. Bruynseraede, *Phys. Rev. Lett.* **76**, 479 (1996).
14. C. Schönberger, A. Bachtold, C. Strunk, J.-P. Salvetat, and L. Forro, *Applied Physics A* **69**, 283 (1999); A. Bachtold, C. Strunk, J.-P. Salvetat, J.-M. Bonard, L. Forro, T. Nussbaumer, and C. Schönberger, *Nature* **397**, 673 (1999).
15. G.-L. Ingold and Yu.V. Nazarov, in: *Single Charge Tunneling*, ed. H. Grabert and M.H. Devoret, (Plenum Press, N.Y., 1992), pp. 21-107.
16. L.S. Levitov, A.V. Shytov, *JEPT Lett.* **66**, 215 (1997).
17. K.A. Matveev and L.I. Glazman, *Phys. Rev. Lett.* **70**, 990 (1993).
18. R. Egger, *Phys. Rev. Lett.* **83**, 5547 (1999); R. Egger and A.O. Gogolin, cond-mat/0101246
19. E.B. Sonin, to be published in *JLTP* July 2001.
20. B.L. Altshuler and A.G. Aronov, *Zh. Eksp. Teor. Fiz.* **77**, 2028 (1979) [*Sov. Phys. JEPT.* **50**, 968 (1979)]; B.L. Altshuler, and A.G. Aronov, in *Electron-Electron Interactions in Disordered Systems*, edited by A.L. Efros and M. Pollak (Elsevier Science Publishers B.V., Amsterdam, 1985).
21. E.G. Mishchenko, A.V. Andreev and L.I. Glazman, cond-mat/0106448.
22. F. Pierre, H. Pothier, P. Joyez, N.O. Birge, D. Esteve, and M.H. Devoret. *Phys. Rev. Lett.* **86**, 1590 (2001).
23. A.D. Zaikin, and D.S. Golubev, these proceedings.
24. D. Chouvaev, L.S. Kuzmin, D.S. Golubev and A.D. Zaikin, *Phys. Rev. B* **59**, 10599 (1999).